

Latest results from RHIC

Experimental evidence for new physics

David J. Hofman

Physics Department, University of Illinois at Chicago, Chicago, IL, 60607, USA

Received: 26 November 2003 / Accepted: 12 December 2003 /
 Published Online: 17 December 2003 – © Springer-Verlag / Società Italiana di Fisica 2003

Abstract. Some of the most recent results from the Relativistic Heavy Ion Collider (RHIC) are reported. Exciting new experimental features have been observed in data from all four experiments. These new observations indicate the creation of a new form of ‘hot dense matter’ at RHIC energies, the properties of which are now beginning to be determined.

PACS. 25.75.-q Relativistic heavy-ion collisions – 25.75.Nq Quark-gluon plasma production

1 Introduction

The Relativistic Heavy Ion Collider (RHIC), located at Brookhaven National Laboratory, is currently the world’s highest energy collider dedicated to providing collisions of heavy ions and the study of the resulting high energy-density matter. Center-of-mass collision energies at RHIC start at $\sqrt{s_{NN}} = 19.6$ GeV, slightly above the highest equivalent energy reached by the fixed target experiments at the CERN-SPS, and reaching a maximum energy of $\sqrt{s_{NN}} = 200$ GeV for $Au + Au$ heavy-ion collisions.

Detailed theoretical calculations, as well as more simplistic arguments, point to the likely formation of a new form of matter at temperatures above the pion mass, at about 170 MeV. In terms of energy-density, it has also been predicted this new form of matter will occur around $0.7 \text{ GeV}/\text{fm}^3$, or about $5 \times$ that of normal nuclear matter ($\epsilon_0 \approx 0.135 \text{ GeV}/\text{fm}^3$). The hope of high-energy heavy-ion physicists is that this new form of matter would be a state where the normal QCD vacuum, a condensate, would ‘melt’ into a type of plasma where quarks (and gluons) are freed from confinement. This deconfined state of the QCD vacuum, in which quarks and gluons are the relevant degrees of freedom, is often referred to as a ‘quark gluon plasma’. Theoretically, QCD tells us this quark gluon plasma would be a state in which chiral symmetry is restored and the quark masses would approach the ‘bare’ (small) values given solely by their interaction with the Higgs condensate. This very interesting state of matter has likely not existed since the first microseconds after the Big Bang.

The first, and foremost, goal of the research program at RHIC, therefore, has been to establish if clear signatures of either a quark gluon plasma or any other new form of matter exist. A detailed study of any such signa-

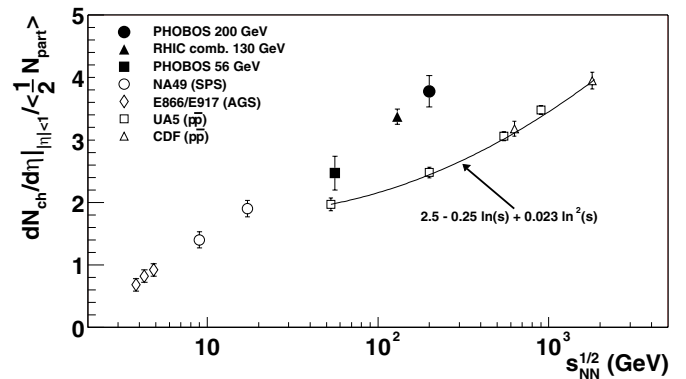


Fig. 1. Excitation function of midrapidity charged particle yields at RHIC for the 6% most central collisions. Figure taken from [1]

tures would naturally follow. The excitement of the new results from RHIC is that, for the first time since measurements of relativistic heavy-ion collisions began, there is clear evidence of possible new physics.

2 Bulk charged particle production

One of the first measurements at RHIC was the number of charged particles produced in head-on collisions of $Au + Au$ nuclei emitted at $\theta = 90^\circ$ ($\eta = 0$ or midrapidity) to the bombarding axis of the colliding nuclei [1]. This result is shown in Fig. 1, where the measured charged particle yield is shown per participating pair of nucleons in order to compare directly to results from pp and $\bar{p}p$ collisions. Head-on, or central, collisions were chosen to maximize the nuclear overlap volume and thus represent those most likely to create an extended region of hot, dense matter.

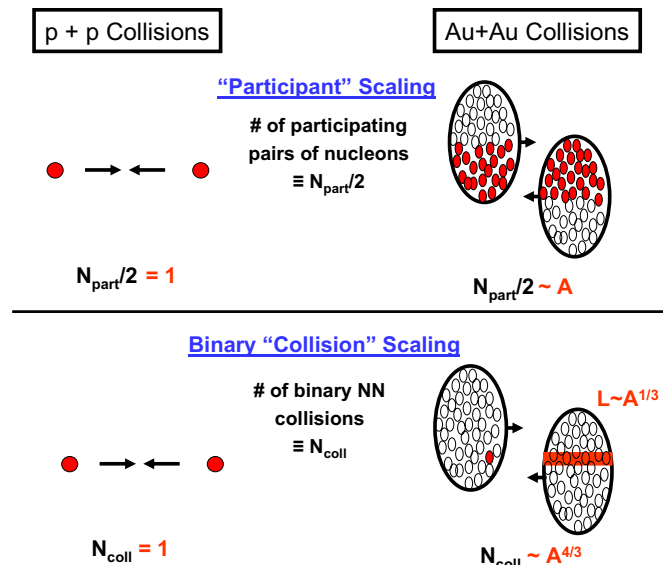


Fig. 2. Illustration of number of participant pairs, $N_{part}/2$, and number of binary collisions, N_{coll} , in $p + p$ vs. $Au + Au$ heavy-ion collisions. In the N_{coll} case for $Au + Au$, each participating nucleon can undergo multiple collisions with nucleons in its path from the other nucleus, as shown above

What is most notable in the heavy-ion data of Fig. 1 is the apparently ‘straight’ exponential scaling of the particle production with collision energy. An additional early surprise was that the yield of charged particles at midrapidity in $Au + Au$ was considerably lower (by up to a factor of two) compared to most of the pre-RHIC theoretical predictions. The yield per participant pair in central $Au + Au$ collisions is still larger, however, than seen in $\bar{p} + p$ collisions at the same energy, indicated by the open squares, triangles and solid curve.

A simple estimate for the energy density achieved at full RHIC energy can be obtained from the measured midrapidity yield for $\Delta\eta = 1$. If we take an average total energy for the particles of $\langle E_{tot} \rangle \approx 1$ GeV, the total particle yield as $dN_{tot}/d\eta \approx 1000$ (i.e. $dN_{ch}/d\eta \approx 650$ at midrapidity [1] and assume roughly an additional 1/3 of the particles are neutrals, mainly π^0 's) and an initial central collision overlap volume of $\pi R^2 \times (1 \text{ fm}) \approx 200 \text{ fm}^3$, one obtains an initial energy density estimate of $\epsilon \approx 5 \text{ GeV}/\text{fm}^3$. This estimate mirrors the value of $\epsilon_{BJ} \approx 4.6 \text{ GeV}/\text{fm}^3$ obtained in a detailed measurement by the PHENIX collaboration at the lower energy of $\sqrt{s_{NN}} = 130 \text{ GeV}$ [4]. This large value of ϵ is significantly above the minimum estimated energy density of $0.7 \text{ GeV}/\text{fm}^3$ for creation of a new form of hot dense matter.

When searching for new physics signals, it is critical to have a baseline of ‘normal’ physics with which to compare the data. This baseline for heavy-ion physics is the equivalent data for pp and $\bar{p}p$ collisions, shown, for example, as the solid line in Fig. 1. The major difference between a $p + p$ vs. a $Au + Au$ collision is the large volume and corresponding range of impact parameters in the heavy-ion case. The large volume and range of impact parameters both give rise to two types of scaling in $Au + Au$

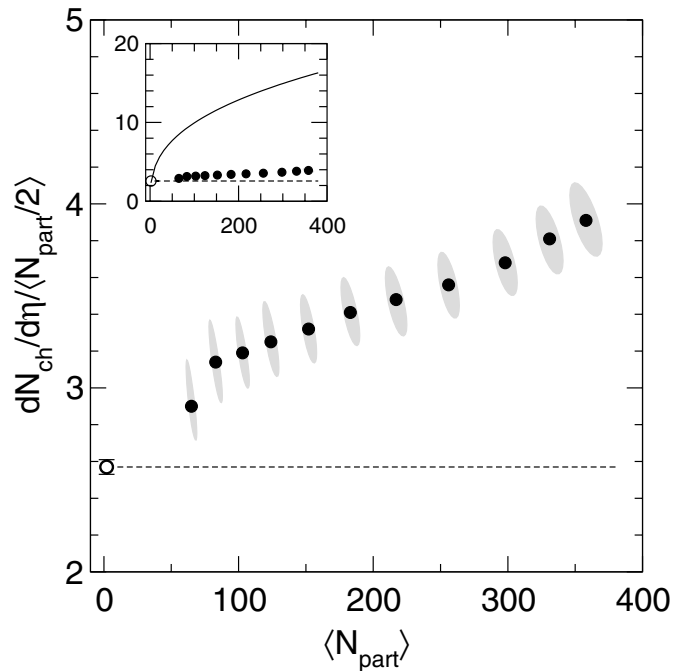


Fig. 3. Centrality, or N_{part} , dependence of the charged particle multiplicity per participant pair at midrapidity for $Au + Au$ collisions at $\sqrt{s_{NN}} = 200 \text{ GeV}$ (solid points). The corresponding $\bar{p} + p$ result is shown as the open point at $\langle N_{part} \rangle = 2$. The inset shows an expanded y-axis scale with the solid line illustrating expectation from N_{coll} binary collision scaling. Data taken from PHOBOS [3]

collisions not present for the $p + p$ case, specifically participant pair ($N_{part}/2$) scaling and binary nucleon-nucleon collision (N_{coll}) scaling as illustrated in Fig. 2.

Determining experimentally the centrality (or impact parameter) of a $Au + Au$ collision is extremely important in the search to understand the underlying collision dynamics. According to a Glauber model calculation, the number of binary collisions, N_{coll} , increases strongly with increasing centrality to the extent that the number of collisions per participant pair of nucleons, $\nu = N_{coll}/(N_{part}/2)$, reaches a value of $\nu \approx 6$ for central $Au + Au$ collisions at full RHIC energy. If the bulk charged particle production in $Au + Au$ collisions were to scale as N_{coll} , it would vary dramatically as a function of increasing centrality and reach very high values for central collisions. This is not what is observed in the data.

The centrality dependence of the mid-rapidity yields in $Au + Au$ collisions as measured by PHOBOS [3] at $\sqrt{s_{NN}} = 200 \text{ GeV}$ are shown in Fig. 3, together with the $\bar{p} + p$ benchmark (open circle and dashed line) and the expectation from binary collision scaling (solid line - see inset). The most dramatic feature of the heavy-ion centrality dependence is that it very closely follows participant pair scaling with only a small ($\approx 10\%$) fraction of N_{coll} scaling allowed by the data [3].

One of the intriguing consequences of the observed flat centrality dependence of midrapidity charged particle yields is that a model based solely on parton saturation

in the colliding nuclei correctly describes the detailed centrality and rapidity dependence of the measured charged particle multiplicities at $\sqrt{s_{NN}} = 130$ and 200 GeV [3, 5, 6]. This model was also one of the few models to correctly predict the low value of the midrapidity charged particle multiplicity for central $Au + Au$ collisions in Fig. 1.

3 New experimental signatures

Due to the exponential nature of the transverse momentum (p_T) spectrum, all measurements of total charged particle multiplicities at midrapidity are dominated by the ‘soft’ particle production at low energy, i.e. $p_T < 1.5$ GeV/c [7]. A bulk charged particle measurement, therefore, solely reflects particle production at low p_T , and it is the low p_T particles that are scaling predominantly as N_{part} . An immediate question is then, what happens at high p_T , where production rates can be calculated using perturbative QCD. These rates are naïvely expected to scale as they do for pp and $\bar{p}p$ collisions, i.e. as N_{coll} , the number of binary nucleon-nucleon collisions. The high p_T particles are also, by necessity, produced in the initial stages of the collision when hard collisions are still possible.

3.1 Charged particle production at high p_T

All four experiments at RHIC have the ability to measure the p_T dependence of charged particle production. Some differences in phase space coverage exist, but a large overlap allows for experimental cross-checks of the results.

The exponential nature of the measured p_T distributions requires a reference for comparison if one is to clearly identify features in the spectrum. The reference spectrum used is from pp and $\bar{p}p$ collisions, leading to the definition of the ‘nuclear modification factor’;

$$R_{AA}(p_T) \equiv \frac{(1/N_{coll})d^2N^{AA}/dp_Td\eta}{(1/\sigma_{inel}^{pp})d^2\sigma^{pp}/dp_Td\eta}.$$

At high momentum ($p_T > 2$ GeV) this ratio should approach unity if the corresponding collisions are scaling as independent binary nucleon-nucleon collisions. In fact, at lower collision energies this ratio was observed to be larger than given by N_{coll} scaling as shown in Fig. 4 by the band of solid lines labeled ‘Pb+Pb(Au) CERN-SPS’. The enhancement above N_{coll} scaling was also observed in lower energy fixed-target p +Nucleus collisions, and is interpreted as being caused by multiple scattering during the initial stages of collision.

The first results from RHIC for R_{AA} in $Au + Au$ collisions at $\sqrt{s_{NN}} = 130$ GeV were surprising, striking and exciting [8]. First, it was observed that the spectral shape in $Au + Au$ collisions was dramatically different from that seen in the reference $p+p$ data. Secondly, at high p_T it was found that R_{AA} did not approach or exceed N_{coll} scaling, but remained significantly suppressed (see solid squares of Fig. 4). This observation, first reported by PHENIX, was

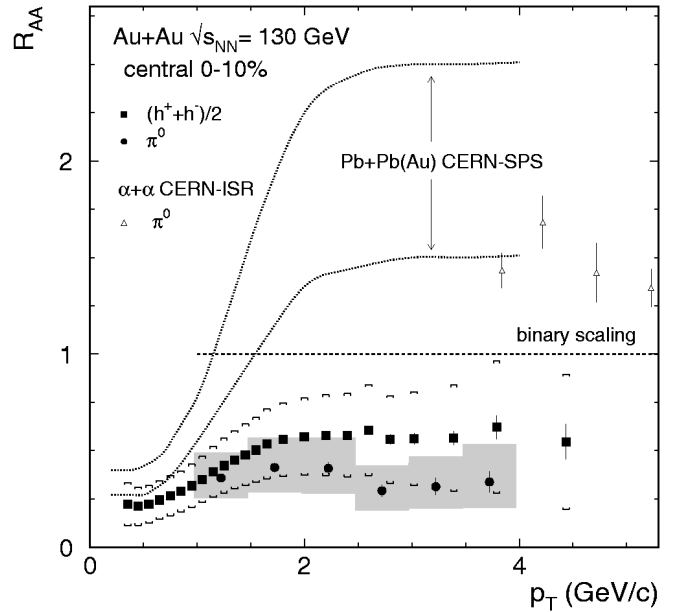


Fig. 4. Comparison of RHIC data for central $Au+Au$ collisions at $\sqrt{s_{NN}} = 130$ GeV to lower energy CERN SPS data. Figure from PHENIX [8]

later confirmed by the other three experiments, who also noted that the degree of high p_T suppression was strongly centrality dependent [7, 9, 10]. The STAR collaboration recently reported the p_T dependence of the ratio of central to peripheral charged particle yields in $Au + Au$ collisions at $\sqrt{s_{NN}} = 200$ GeV, which showed a strong ($\sim 5\times$) suppression below binary collision scaling up to p_T values of 11 GeV/c [11].

There are currently two principle approaches to understanding the suppression of high p_T particles in central $Au + Au$ collisions. The first approach utilizes pQCD to calculate the initial high p_T production rates coupled with a large partonic energy loss in a dense medium to reduce the yield to experimental values [12, 13, 14, 15]. In this picture, a produced dense medium of sufficient volume is only created in central $Au + Au$ collisions, and it is the energy loss incurred by interaction of high energy partons through this dense medium that is responsible for the experimental effect. It is therefore sometimes referred to as a ‘final state’ effect [11]. The second approach utilizes the same parton saturation picture that was successful in describing the yields and angular distributions of bulk charged particle multiplicities [5, 6, 16]. This model also describes the dearth of high p_T particles through parton saturation in the wavefunctions of Au nuclei, i.e. the colliding Lorentz contracted Au nuclei are not simple linear superpositions of individual nucleons. If parton saturation is responsible for the observation, then the experimental effect would be solely an ‘initial state’ effect [11] and not be due to partonic energy loss in a new form of matter.

The most recent run at RHIC was designed to provide additional experimental information that may help clarify this understanding. RHIC ran collisions of $d + Au$ at the equivalent collision energy of $\sqrt{s_{NN}} = 200$ GeV in order to

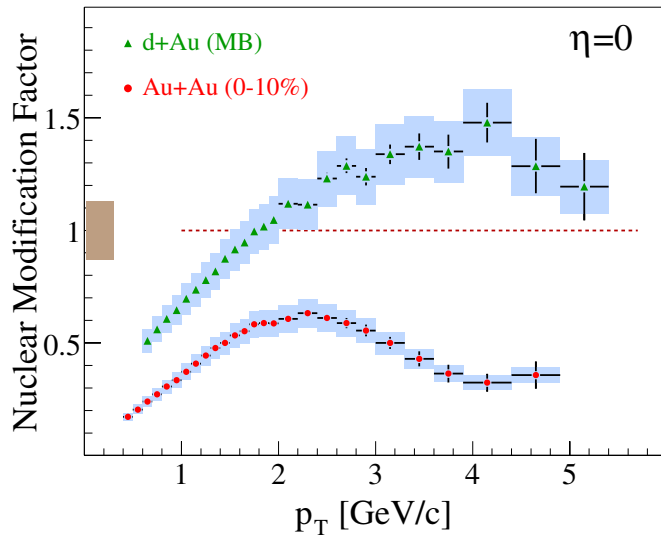


Fig. 5. Plot of the nuclear modification factor, R , for charged particles in minimum bias (MB) $d + Au$ and 0-10% central $Au + Au$ collisions at $\sqrt{s_{NN}} = 200$ GeV. The $d + Au$ data at midrapidity do not show evidence of high p_T suppression relative to N_{coll} scaling. Figure from BRAHMS [17]

provide a situation in which the “initial state” of one colliding Au nucleus was not changed, but due to the much smaller size of the d , no large volume of hot and dense matter could be created. One might therefore expect that this experimental situation could aid in differentiating between “initial” and “final” state effects in the suppression of high p_T particles.

The results from the $d + Au$ measurements are illustrated in Fig. 5 with data from the BRAHMS collaboration [17]. All four experiments observed similar effects [17, 18, 19, 20]. The strong suppression below N_{coll} scaling of high p_T particle yields in central $Au + Au$ collisions is not present in either inclusive $d + Au$ [17, 18, 19] or central $d + Au$ [20] data. Predictions (before the experiments were completed) from the parton saturation model indicated that for central $d + Au$ collisions one might still expect some suppression of high p_T particles [16], which was not seen in data.

3.2 Neutral π^0 production at high p_T

A unique capability of the PHENIX experiment is the ability to measure neutral π^0 yields via the $\gamma\gamma$ decay branch through use of calorimetry. The calorimeters are situated at midrapidity and cover $\Delta\phi = \pi$ in azimuth. Two separate types of calorimeters, PbSc and PbGl, were utilized, and data taken by both types was separately analyzed.

The resulting nuclear modification factor for $d + Au$ and $Au + Au$ central collisions is shown in Fig. 6. The two independent analyses for inclusive $d + Au$ collisions agree within systematics, and show a scaling that is consistent with, or slightly above, N_{coll} scaling. The $d + Au$ result is in stark contrast to the central $Au + Au$ data that

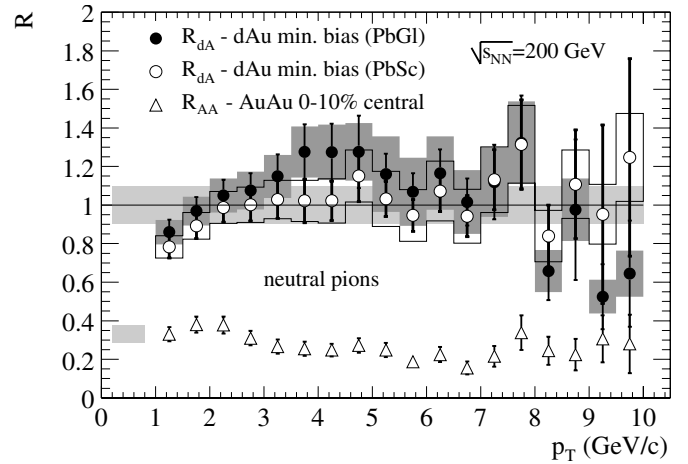


Fig. 6. The nuclear modification factor, R , for π^0 yields in inclusive (min. bias.) $d + Au$ and central $Au + Au$ collisions. Figure from PHENIX [18]

is strongly suppressed relative to N_{coll} scaling (shown as open triangles in Fig. 6).

The central feature seen in the p_T dependence of both charged particle emission and neutral π^0 emission at midrapidity is suppression of the nuclear modification factor, R , below N_{coll} scaling for central $Au + Au$ collisions and no suppression for $d + Au$ collisions.

3.3 Back-to-back jet emission

A unique capability of the STAR experiment is detailed event characterization measurements using their large acceptance ($|\eta| \leq 1.8$, $\Delta\phi = 2\pi$) Time Projection Chamber for tracking and particle identification. Of particular interest to this report is the use of the detector to study event-by-event two-particle correlations between high p_T particles, i.e. jets or jet-like events. Planarity is approximately enforced by only including particles within $|\eta| < 0.7$ in the analysis. Two-particle azimuthal distributions are created where the correlation in azimuthal angle ϕ is formed between high p_T tracks in the range of $4 < p_T(\text{trig}) < 6$ GeV/c and all associated tracks in the same event having $2 < p_T < p_T(\text{trig})$. The resulting distribution, $(1/N_{\text{trigger}}) \times dN/d(\Delta\phi)$, is then formed for each event, corrected for tracking efficiency, and summed over all events selected in the sample [19].

The expectation for this high p_T azimuthal two-particle correlation in $p + p$ collisions would be a ‘nearside’ peak at $\Delta\phi \approx 0$, typical of jet production, and a back-to-back ‘farside’ peak at $\Delta\phi \approx \pi$ typical of di-jet events. The result for $p + p$ collisions is shown in both panels of Fig. 7 as the solid line histogram. The clear peaks in the $p + p$ data at $\Delta\phi \approx 0$ and π follow exactly this expectation for both ‘nearside’ and ‘farside’ events from jets and di-jets.

The results for central $Au + Au$ collisions are shown as the stars in Fig. 7b. The ‘nearside’ peak at $\Delta\phi = 0$ is still present, but the ‘farside’ peak at $\Delta\phi = \pi$ is no longer apparent. It is important to note that the ‘farside’

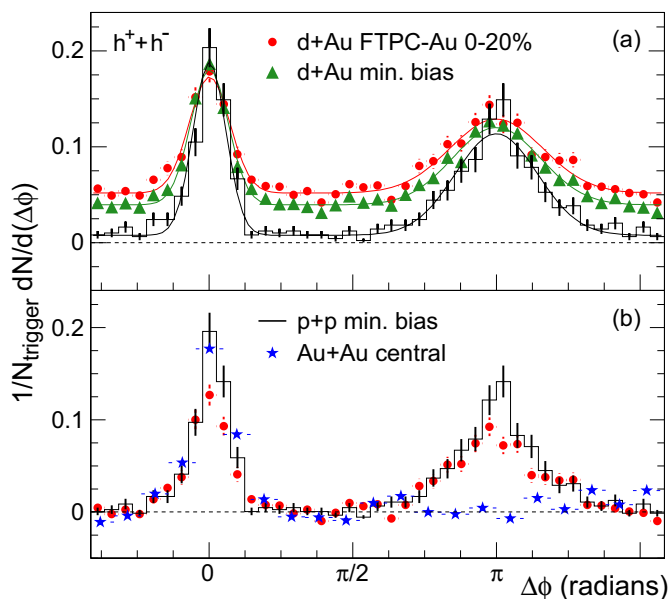


Fig. 7. Two-particle azimuthal distributions for high p_T particles in $p + p$, $d + Au$ and central $Au + Au$ collisions at $\sqrt{s_{NN}} = 200$ GeV. See text for details. Figure from STAR [19]

peak absent in central $Au + Au$ collisions is recovered for peripheral $Au + Au$ collisions, as detailed in [21].

The disappearance of the ‘farside’ peak for central $Au + Au$ collisions is another dramatic experimental result pointing to possible new physics at RHIC. The experimental data can be understood most intuitively as a direct consequence of a large partonic energy loss of high p_T particles in dense matter that acts to suppress one of the two di-jets passing through the largest amount of matter. Parton saturation in the colliding nuclei, however, may also be able to account for the observation through an effective reduction of the number of di-jet events produced in the initial state through the mechanism of an increased mono-jet contribution [22].

STAR analyzed the recent data from $d + Au$ collisions at RHIC in the same manner as $p + p$ and $Au + Au$. The results of this analysis are given as the solid points in Fig. 7a,b for central $d + Au$ collisions. For the $d + Au$ case, the ‘farside’ di-jet events that are missing in central $Au + Au$ collisions are present. This behavior mirrors the high p_T suppression detailed in Sect. 3.1 and 3.2, and led the STAR collaboration to conclude that the data from central $Au + Au$ collisions are due to final-state interactions with the dense medium produced in the collision [19].

Although the $d + Au$ data does seem, at this stage, to disfavor the saturation model as the sole explanation for both high p_T and di-jet suppression in central $Au + Au$ collisions, it is important to make the same measurements away from midrapidity where the effects of saturation on the observed suppression are expected to increase [23].

4 Conclusion

The four experiments at RHIC have found exciting experimental evidence for new physics. The evidence is based on very clear signatures that are manifest solely in central $Au + Au$ collisions and diminish or vanish entirely for peripheral $Au + Au$ collisions as well as for $p + p$ and $d + Au$ collisions. The current understanding is that the data indicate creation of a hot dense matter in these central $Au + Au$ collisions. The details of the mechanism responsible for creation of this matter are still under investigation.

This work was supported in part by U.S. DOE grant DE-FG02-94ER40865.

References

1. PHOBOS Collaboration (B.B. Back et al.): Phys. Rev. Lett. **85**, 3100 (2000), Phys. Rev. Lett. **88**, 22302 (2002)
2. PHOBOS Collaboration (B.B. Back et al.): Phys. Rev. Lett. **91**, 052303 (2003)
3. PHOBOS Collaboration (B.B. Back et al.): Phys. Rev. C Phys. **65**, 061901(R) (2002)
4. PHENIX Collaboration (K. Adcox et al.): Phys. Rev. Lett. **87**, 052301 (2001)
5. D. Kharzeev and M. Nardi: Phys. Lett. B **507**, 121 (2001)
6. D. Kharzeev and E. Levin: Phys. Lett. B **523**, 79 (2001)
7. PHOBOS Collaboration (B.B. Back et al.): Phys. Lett. B (2003) in press, [arXiv:nucl-ex/0302015]
8. PHENIX Collaboration (K. Adcox et al.): Phys. Rev. Lett. **88**, 022301 (2002)
9. STAR Collaboration (C. Adler et al.): Phys. Rev. Lett. **89**, 202301 (2002)
10. BRAHMS Collaboration (I. Arsene et al.): Phys. Rev. Lett. (2003) in press, [arXiv:nucl-ex/0307003]
11. STAR Collaboration (J. Adams et al.): Phys. Rev. Lett. **91**, 172302 (2003)
12. M. Gyulassy and X.N. Wang: Nucl. Phys. B **420**, 583 (1994)
13. X.N. Wang: Phys. Rev. C **58**, 2321 (1998)
14. I. Vitev and M. Gyulassy: Phys. Rev. Lett. **89**, 252301 (2002)
15. M. Gyulassy, I. Vitev, X.N. Wang, and B. Zhang: arXiv:nucl-th/0302077
16. D. Kharzeev, E. Levin, and L. McLerran: Phys. Lett. B **561**, 93 (2003)
17. BRAHMS Collaboration (I. Arsene et al.): Phys. Rev. Lett. **91**, 072305 (2003)
18. PHENIX Collaboration (S.S. Adler et al.): Phys. Rev. Lett. **91**, 072303 (2003)
19. STAR Collaboration (J. Adams et al.): Phys. Rev. Lett. **91**, 072304 (2003)
20. PHOBOS Collaboration (B.B. Back et al.): Phys. Rev. Lett. **91**, 072302 (2003)
21. STAR Collaboration (C. Adler et al.): Phys. Rev. Lett. **90**, 082302 (2003)
22. D. Kharzeev: Nucl. Phys. A **715**, 35c (2003)
23. D. Kharzeev, Y.V. Kovchegov, and K.Tuchin: arXiv:hep-ph/0307037